XVI SIMPOSIO
IBEROAMERICANO
SOBRE PROTECCIÓN
DE SISTEMAS ELÉCTRICOS
DE POTENCIA

Fault Location for Multi-terminal Lines

Jörg Blumschein[a], Cezary Dzienis[b], Jens Hauschild[c]

[a]*Siemens AG, Smart Infrastructure Division*
[b]*University of Applied Sciences Zittau/Görlitz*
[c]*50Hertz Transmission GmbH*

A B S T R A C T

Worldwide there is a trend to increase the use of renewable energy to replace the conventional energy sources as far as possible. Beside small installations like photovoltaics panels on rooftops of private homes we can observe big wind and photovoltaics or solar farms supplying significant amounts of electrical power into the grid.

These big wind, photovoltaics and solar power plants are not seldom directly connected to existing transmission or distribution lines. In this case we get transmission lines with three or more terminals.

These multi-terminal lines with significant intermediate infeed are a challenge for the protection but also challenging for the exact location of the fault. Reliable localization of short circuit in the power system network is important for the safe management of power grids. For solid earthed networks technologies for a sufficiently accurate location of the fault are available. They are implemented in protection devices or are available in form of the higher-level fault location system monitoring bigger network areas. For these both philosophies, the fault location is performed by the evaluation of the determined short circuit reactance at fundamental frequency. An improvement of the fault location result can be achieved by double-ended algorithm. However, these two methods require an effective measurement window of at least one period, which is a certain limitation for a more accurate fault location especially for short-term faults. In addition, these approaches are successfully applied only for lines with two terminals, what provide some limitations for lines including intermediate infeed as a case of solar and wind farms direct connected to the lines. Therefore, some extensions in algorithms are necessary to apply conventional fault location for multi-terminal lines. Intensive investigation in the last years in area of a fault location showed that the usage of the travelling wave phenomena can be a promising solution for some problematic network configurations. To assess if reliable results can be achieved and which limitations occur, this technology was implemented in different grids and voltage levels: 110 kV compensated, 400 kV and 525 kV solid earthed networks. From these investigations it was concluded, that travelling wave technology could be one of the possible solutions on the field of fault location for multi-terminal lines.

This paper introduces typical topologies of multi-terminal lines. Based on these topologies and gathered experiences from network operator installations, the impact of different approaches of fault location, like impedance-based methods or travelling wave methods, on the fault location error is discussed. This paper presents both real and simulated cases, with detailed analysis of error sources. Finally, suggestions are given how to implement an optimal fault locator approach for multi-terminal lines.

Keywords: Fault location, impedance calculation, travelling wave, multi-terminal lines

1. Multi-terminal lines

In most cases multi-terminal lines did not result from the initial planning, Often, multi-terminal lines result from the need to connect new generation or load to the power system without building new lines or substations.

A typical topology is shown in Fig. 1. Initially a line was built to connect substation A with substation B. Later new generation or load centre like for instance wind farms, represented by substation C, D and E needed to be connected to the system. Substation C and D are far away from the existing substations A and B but close to the line, connecting substation A and B. For that reason, it is an economical and fast solution to build lines from substations C and D and tap these lines to the existing line connecting substation A and B. For new substations closer to existing substations, like substation E in figure 1 which is close to substation B the advantages of tapping the line are less. That's why such substations are mostly directly connected to the existing substations. In other words, it is more likely that taps

are connected in the middle of an existing line like substation C and D in Fig. 1.

2. Single-ended impedance-based fault location

Single-ended impedance-based fault location is the most common method of fault location. This method has the great advantage that only measurements from the local end of a line are needed. The method estimates the fault location by calculating the apparent impedance $\mathbf{Z}_{\text{App}}$ using the voltage $\mathbf{U}_A$ and the current $\mathbf{I}_A$ measured at the relay location like shown in Fig. 2.

Single-ended impedance-based fault location is calculating the apparent impedance $\mathbf{Z}_{\text{App}}$ according to Ohm's law:

$$\mathbf{Z}_{\text{App}} = \frac{\mathbf{U}_A}{\mathbf{I}_A} \tag{1}$$

$\mathbf{Z}_{\text{App}}$ = apparent impedance, measured at substation A.

$\mathbf{U}_A$ = voltage, measured at substation A.

$\mathbf{I}_A$ = current, measured at substation A.

If the fault is located between the local terminal and the T-Point a fault location is possible considering the normal impacting factors for single-ended impedance-based fault location[1].

- Effect of load current and fault resistance
- Inaccurate fault type identification
- Zero sequence mutual effects
- Uncertainties about line parameters
- Accuracy of the line model like transpositions
- Shunt reactors and capacitors
- Load flow unbalance
- Series compensation
- Measurement errors
- Measuring window position
- Sampling rate

However, if the fault is between the T-Point and a remote terminal as shown in Fig. 3, a single-ended fault location using voltages and currents from the local terminal cannot give the correct fault location. There are at least two problems:

1) Using only local measurements from terminal A it is not possible to estimate whether the fault is between the T-Point and terminal B or between the T-Point and terminal C.
2) For a fault behind the T-Point the infeed or outfeed from the third terminal can produce an inacceptable measurement error[2].

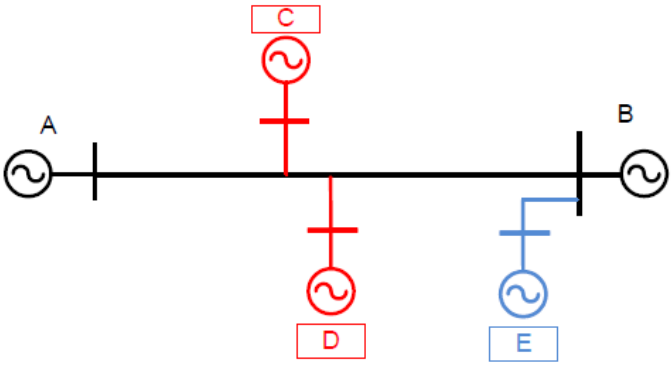

Fig. 1. Single line diagram representing a four-terminal line

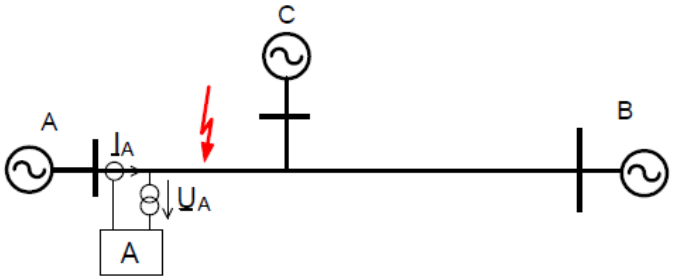

Fig. 2. Single line diagram for a fault between station A and the T-Point of a three-terminal line.

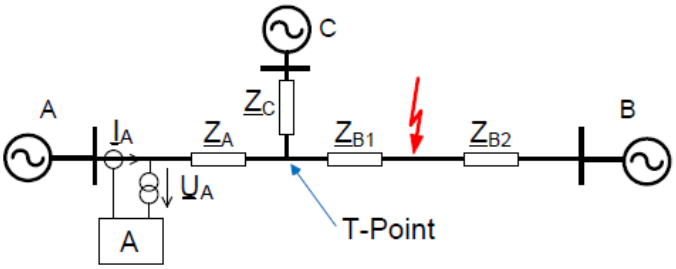

Fig. 3. Single line diagram for a fault behind the T-Point of a three-terminal line.

For a bolted fault between the T-Point and terminal B like shown in Fig. 3 the apparent impedance can be calculated according to

$$\mathbf{Z}_{\text{App}} = \frac{\mathbf{U}_A}{\mathbf{I}_A} = \mathbf{Z}_A + \mathbf{Z}_{B1}\frac{\mathbf{I}_A + \mathbf{I}_C}{\mathbf{I}_A} \tag{2}$$

$\mathbf{Z}_A$ = line-impedance between substation A and T-Point.

$\mathbf{Z}_{B1}$ = line-impedance between T-Point and fault.

$\mathbf{I}_C$ = current contribution from substation C.

The measurement error, introduced by the infeed from terminal C can be calculated according to

$$\mathbf{Z}_{\text{Error}} = \mathbf{Z}_{B1}\frac{\mathbf{I}_C}{\mathbf{I}_A}. \tag{3}$$

$\mathbf{Z}_{\text{Error}}$ = impedance error due to the infeed from substation C.

From (3) we can conclude that the measurement error for the single-ended impedance-based fault location depends on the relation of the local current $\mathbf{I}_A$ compared to the current contribution $\mathbf{I}_C$ from the remote terminal C.

This means that the result of single-ended impedance-based fault location for faults behind the T-Points is only useful if the infeed from the local side is high compared to the remote infeed.

3. Double-ended fault location

Double-ended fault locators calculate the distance to fault using measurements from two ends of a line. By using voltages and currents from both ends of the line several problems of the single-ended fault location can be solved.

A common method for double-ended fault location is using voltage profiles along the line. According to Fig. 4 the voltage profile $U_{A\rightarrow B}$ is calculated using voltages and currents from terminal A and voltage profile $U_{B\rightarrow A}$ is calculated using voltages and currents from terminal B. In this example the negative sequence voltage is used.

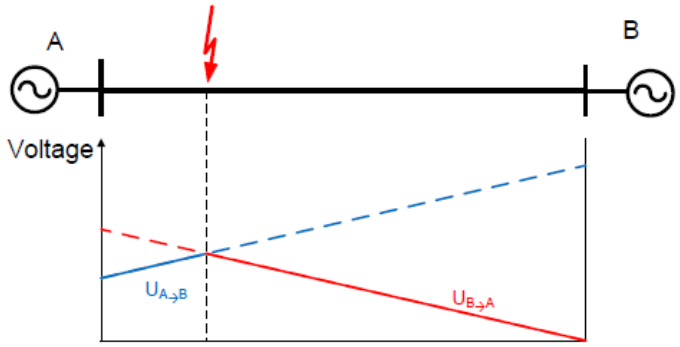

Fig. 4. Voltage profiles calculated from both ends of the line.

The fault location is the point where both voltage profiles intersect.

This method of double-ended fault location has the following advantages compared to the single-ended impedance-based method[3].

- Immune against load flow, remote infeed, and fault resistance.
- No impact of mutual coupling from the parallel line.
- No impact of inaccuracy of residual current compensation factor.

Fig. 5 shows a three-terminal line with a fault between the T-Point and terminal C. Below the single line diagram it shows the voltage profiles for the unfaulted branches of a three- terminal line. In this case the intersection of both voltage profiles is measured at the T-Point of the three-terminal line.

Fig. 6 shows the voltage profiles including the faulted branch of the three-terminal line. In this case the intersection of the voltage profile calculated from terminal A and terminal B does not give the fault location. This is because the voltage profile changes at the T-Point due to the infeed coming from terminal C.

Tziouvaras *et al.* give a solution for this problem[4]. Based on the voltages and currents from terminal B and terminal C the voltage and current at the T-Point can be calculated.

Using the calculated voltage and current at the T-Point the voltage profile $U_{\text{T-Point}\to A}$ can be estimated. The intersection of this voltage profile $U_{\text{T-Point}\to A}$ with the voltage profile $U_{A\to B}$ gives the correct fault location like shown in Fig. 6.

4. Travelling wave fault location

Due to recent advantages in technology travelling waves originated by faults becomes more attractive for fault location. Several methods

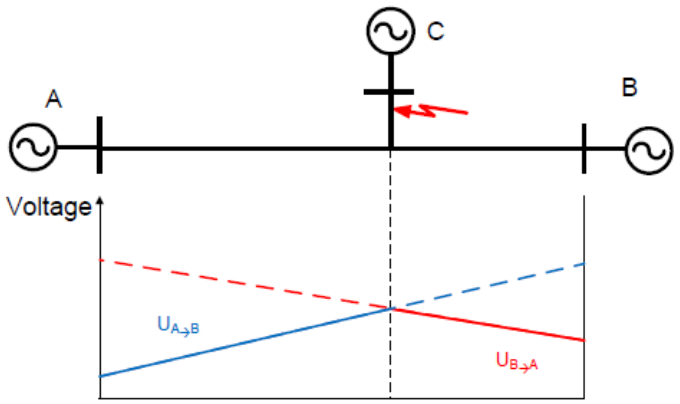

Fig. 5. Voltage profiles for the unfaulted branches of a three-terminal line.

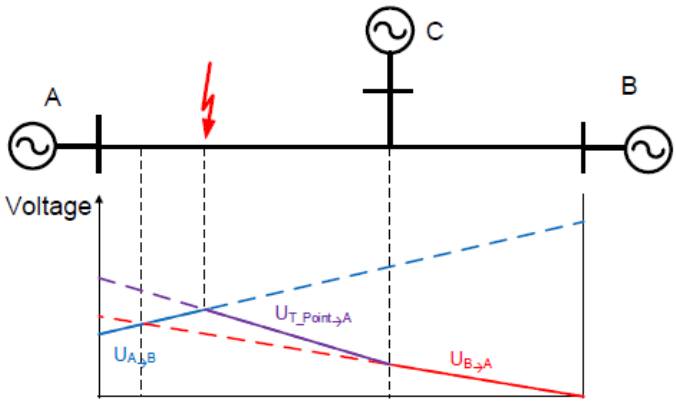

Fig. 6. Voltage profiles including the faulted branch for a fault on a three-terminal line.

of travelling wave fault location exists. In this paper we will consider single-ended and double-ended passive methods with respect to the application for multi-terminal lines.

The principle of single-ended and double-ended passive methods of travelling wave fault location can be explained using an example shown in Fig. 7.

A fault between terminal A and the T-Point of the three terminal line causes travelling waves which are propagating with nearly the speed of light in both directions.

As the fault shown in Fig. 7 is quite close to terminal A the travelling wave reaches terminal A first at t_{A1}. At terminal A the travelling wave gets reflected to the fault and from the fault it gets reflected again back to terminal A where it will be received at t_{A2}.

At the same time another travelling wave propagates in direction to terminal B and terminal C. At the T-Point this wave splits and one wave propagate to terminal B and another wave propagates to terminal C. In this example the wave to terminal C is faster and reaches terminal C at t_{C1}, later the wave to terminal B reaches terminal B at t_{B1}. Both waves get reflected at terminal B and C and propagate back to terminal A.

Finally at terminal A different waves are received at t_{A1} to t_{A6} and it can be quite complicated to find the right one for the single-ended fault location.

Please note that the Bewley's Lattice Diagram in Fig. 7 is a simplification because it seems that the wave to terminal B is propagating via

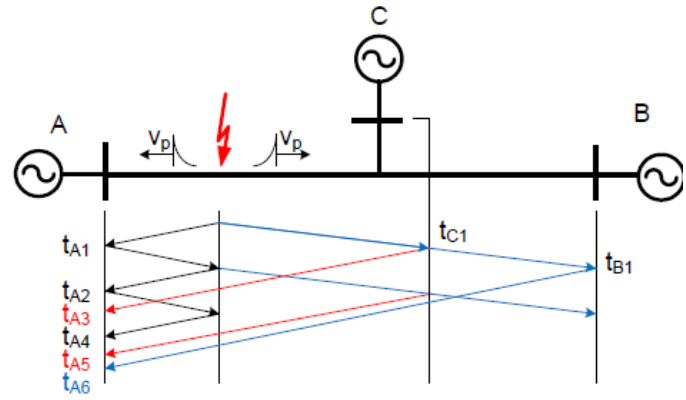

Fig. 7. Travelling waves and its reflections for a fault between terminal A and the T-Point of a three-terminal line.

terminal C which is not the case according to the single line diagram. Related to the given times t_{B1} and t_{C1} there is no influence if the propagation time is the same on the branches from the T-Point to terminal B and terminal C.

4.1. Single-ended method

The single-ended passive method calculates the fault location by the time difference between the arrival of the initial wave front and the reflections from the fault according to

$$D_{\text{Fault}} = v_p \frac{\Delta t}{2} \tag{4}$$

D_{Fault} = distance to fault.
v_p = propagation velocity of the travelling wave.
Δt = time difference in the arrival of the initial wave and the first reflection from the fault.

The single-ended passive method works very well if the fault is close to the local terminal. In this case it is easy to identify the first refection or even several reflections from the fault.

Fig. 8 shows a travelling wave record for a fault in phase C close to the local terminal. This record shows the initial travelling wave and several reflections from the fault. The magnitude of the reflections is decreasing but the time difference between the reflections Δt is constant approximately 70 µs in this example. This corresponds to a fault location of approximately 10 km according to formula (4).

If the fault is close to the T-Point or even behind there will be several reflections from different points and it can be hard to identify which one is the first reflection from the fault.

4.2. Double-ended method

The double-ended passive method calculates the fault location by the time difference between the arrival of the initial wave front at different terminals according to

$$D_{\text{Fault}} = \frac{L}{2} + v_p \frac{\Delta t}{2} \tag{5}$$

D_{Fault} = distance to fault.
L = length of the line between both terminals.
v_p = propagation velocity of the travelling wave.
Δt = time difference in the arrival of the initial wave and the first reflection from the fault.

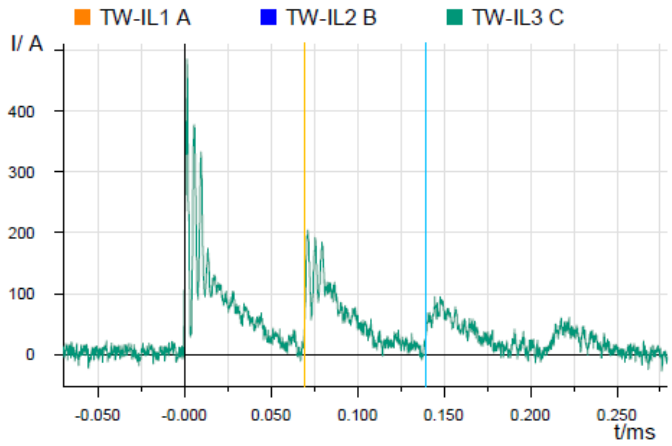

Fig. 8. Initial travelling wave and its reflections for a fault close to the terminal.

Fig. 9 shows the propagation of the initial travelling waves caused by a fault between terminal A and the T-Point of a three-terminal line.

The travelling wave propagating to terminal A reaches terminal A at the time t_{A1}. The travelling wave propagating to the opposite direction reaches the T-Point first where it is splits into two parts. The first part reaches terminal C at the time t_{C1}, and finally the second part reaches terminal B at the time t_{B1}.

For the three-terminal line shown in figure 9 the double-ended passive method according to (5) can be applied in three different combinations:

$$D_{\text{Fault A}} = \frac{L_{AB}}{2} + v_p \frac{t_{A1} - t_{B1}}{2} \tag{6}$$

$$D_{\text{Fault A}} = \frac{L_{AC}}{2} + v_p \frac{t_{A1} - t_{C1}}{2} \tag{7}$$

$$D_{\text{Fault C}} = \frac{L_{CB}}{2} + v_p \frac{t_{C1} - t_{B1}}{2} \tag{8}$$

$D_{\text{Fault A}}$ = distance to fault from terminal A.
$D_{\text{Fault C}}$ = distance to fault from terminal C.
L_{AB} = length of the line between terminal A and B.
L_{CB} = length of the line between terminal C and B.
v_p = propagation velocity of the travelling wave.
t_{x1} = arrival time of the initial wave at terminals x.

Considering the fault to be located between terminal A and the T-Point of the line like shown in Fig. 9, (6) and (7) will give the correct fault location. Eq. (8) will deliver the T-Point as the fault location. This is because (5) needs the time difference from two ends of a line including the fault location.

That means double-ended travelling wave fault location works well for multi-terminal lines but only if the faulted segment is already known.

5. Wrong fault location for a 400 kV three-terminal line

In this Section, a real-world case of wrong fault location for a three terminal-line is analysed which happened in the 400 kV system in Germany. Fig. 10 shows the topology of the three- terminal line.

Substation M on the left side is a pumped-storage power plant. At the time the fault happened the line was not connected to substation M. Substation Z in the middle is a weak source, mainly supplying local loads. Substation R on the right side is the main source, connecting this three-terminal line to the main part of the 400 kV system.

The fault was cleared correctly by line differential protection, but the fault location system did not deliver a plausible result. The fault location system estimated a fault 21 km away from substation M. This location could be close to substation Z or on the line segment to substation R like indicated by the yellow arrows in figure 10. A

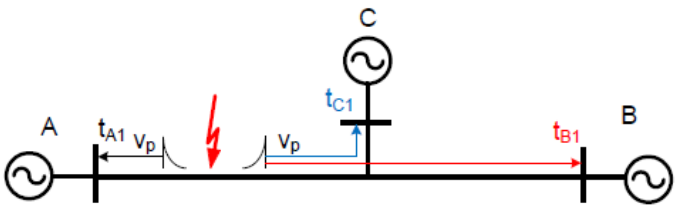

Fig. 9. Initial travelling wave propagating to terminal A, B and C of a three-terminal line.

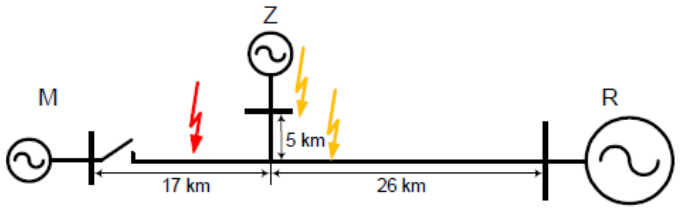

Fig. 10. Topology of the three-terminal line as part of the 400kV transmission system

lightning detection system indicated many lightnings close to the line around 10 km away from substation M at the time of the fault.

Fig. 11 shows the current contribution for this fault. Substation R has the greatest contribution with around 10 kA, substation Z contributes only 0.5 kA and substation M has no contribution.

The single-ended impedance-based fault location estimates the fault location at 60 km from substation Z and 34.9 km away from substation R.

Comparing these results with the topology shown in figure 10 it is obvious that at least one result must be wrong. The result calculated from substation R should be more reliable because the current contribution from substation R is much higher compared to the current contribution from substation Z.

Considering that substation Z estimates a fault far away in forward direction it seems clear that the fault must be located on the branch to substation M.

Fig. 12 shows the line impedances relevant for the single- singleended impedance-based fault location.

For a fault between substation M and the T-Point like shown in Fig. 12 the apparent impedance measured at substation Z can be calculated according to

$$\mathbf{Z}_{\text{App }Z} = \frac{\mathbf{U}_Z}{\mathbf{I}_Z} = \mathbf{Z}_Z + \mathbf{Z}_{M2}\frac{\mathbf{I}_Z + \mathbf{I}_R}{\mathbf{I}_Z} \tag{9}$$

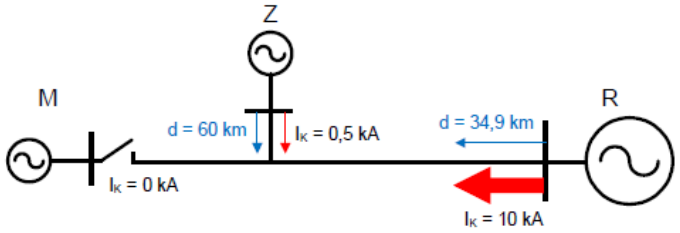

Fig. 11. Current contribution and results of single-ended impedance-based fault location.

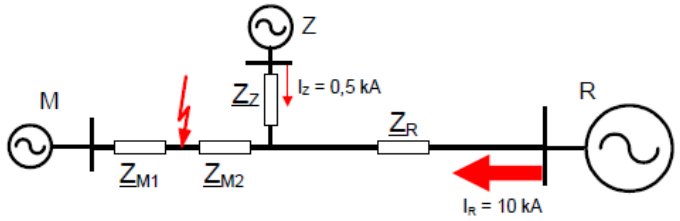

Fig. 12. Impedances relevant for the single-ended impedance-based fault location.

$\mathbf{Z}_{\text{App }Z}$ = apparent impedance measured at substation Z.
$\mathbf{Z}_Z$ = line-impedance between substation Z and T-Point.
$\mathbf{Z}_{M2}$ = line-impedance between T-Point and fault.
$\mathbf{I}_Z$ = current measured at substation Z.
$\mathbf{I}_R$ = current contribution from substation R.

The measurement error, introduced by the infeed from substation R can be calculated according to

$$\mathbf{Z}_{\text{Error }Z} = \mathbf{Z}_{M2}\frac{\mathbf{I}_R}{\mathbf{I}_Z} \tag{10}$$

$\mathbf{Z}_{\text{Error }Z}$ = impedance error due to the infeed from substation R.

From (10) we can conclude that the measurement error for the single-ended impedance-based fault location at substation Z in this case is huge. It is around 20 times the impedance between the T-Point and the fault because the current from the remote substation is 20 times higher compared to the local current.

For the same fault between substation M and the T-Point like shown in Fig. 12 the apparent impedance measured at substation R can be calculated according to

$$\mathbf{Z}_{\text{App }R} = \frac{\mathbf{U}_R}{\mathbf{I}_R} = \mathbf{Z}_R + \mathbf{Z}_{M2}\frac{\mathbf{I}_Z + \mathbf{I}_R}{\mathbf{I}_R} \tag{11}$$

$\mathbf{Z}_{\text{App }R}$ = apparent impedance measured at substation R.
$\mathbf{Z}_R$ = line-impedance between substation R and T-Point.
$\mathbf{Z}_{M2}$ = line-impedance between T-Point and fault.
$\mathbf{I}_Z$ = current measured at substation Z.
$\mathbf{I}_R$ = current contribution from substation R.

The measurement error, introduced by the infeed from substation Z can be calculated according to

$$\mathbf{Z}_{\text{Error }R} = \mathbf{Z}_{M2}\frac{\mathbf{I}_Z}{\mathbf{I}_R} \tag{12}$$

$\mathbf{Z}_{\text{Error }R}$ = impedance error due to the infeed from substation Z.

From (12) we can conclude that the measurement error for the single-ended impedance-based fault location at substation R due to the infeed from substation Z in this case is quite small. It is around 0.05 times the impedance between the T-Point and the fault because the current from substation Z is 20 times lower compared to the local current.

To evaluate the general accuracy of the single-ended impedance-based fault location at substation R Fig. 13 shows the currents and voltages at substation R.

The fault currents at substation R contain a significant DC component and other transients. Due to this the calculated fault impedance depends strongly on the position of the measurement window as shown in Fig. 14.

The impedance trajectory shown in Fig. 14 is based on Fourier filters which are quite sensitive to DC components. The measured impedance differs more than 10%, depending on the position of the measurement window. Special filters can reduce this error, but it is not possible to eliminate it completely.

Fig. 15 shows the result of the single-ended impedance- based fault location. The fault was located 34.9 km away from substation R.

Finally, a double-ended fault location was performed. Unfortunately, only the double-ended fault location between substation Z and substation R could be performed because at substation M the line was not connected at the time of fault. Fig. 16 shows the result of the double-ended fault location.

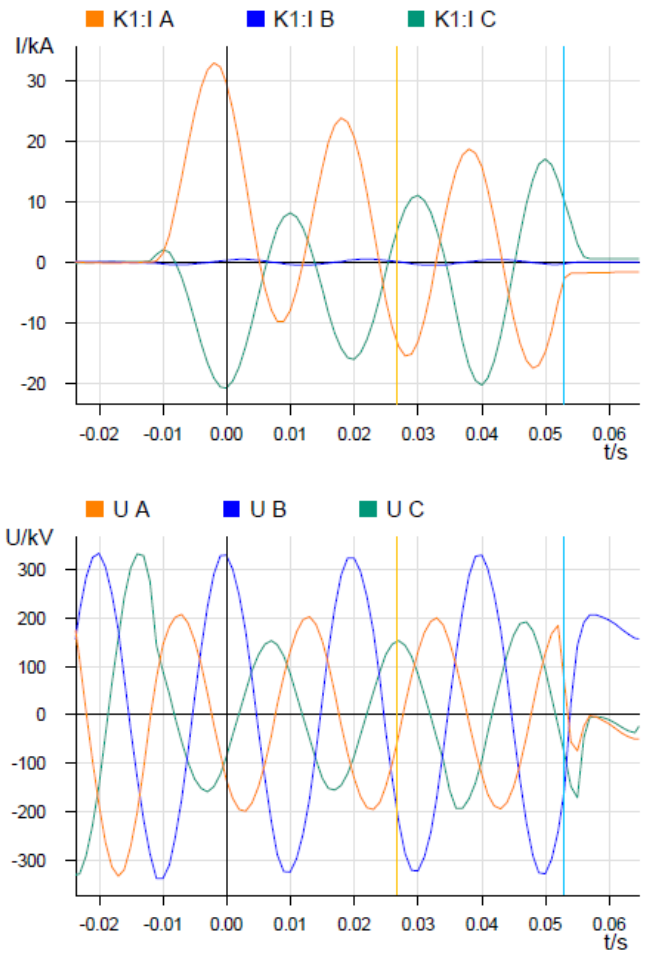

Fig. 13. Fault currents and voltages at substation R.

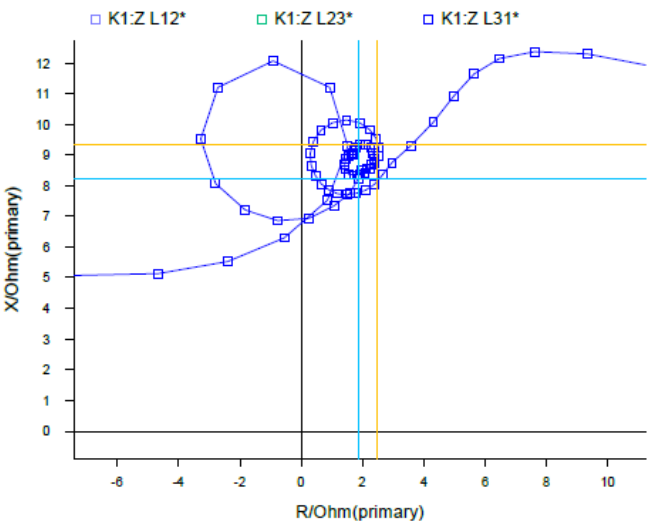

Fig. 14. Impedance trajectory at substation R.

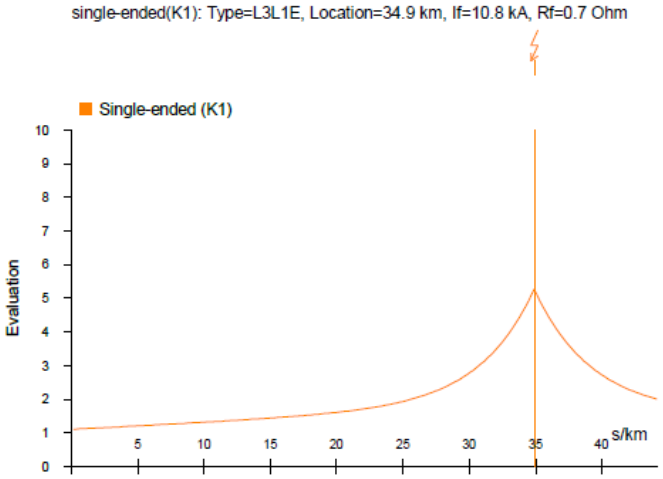

Fig. 15. Result of single-ended fault location at substation R.

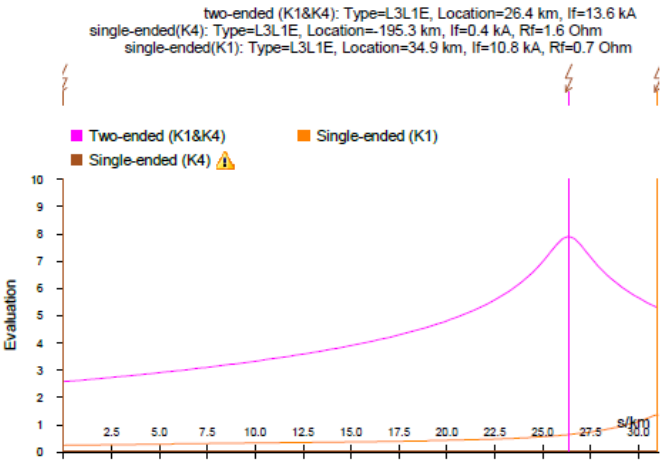

Fig. 16. Result of double-ended fault location between substation R and Z.

The result of the double-ended fault location using data from substation Z and substation R was a fault at 26.4 km away from substation R. This is very close to the T-Point of the line which was the expected result.

6. Conclusion

It was shown that there is no single method for optimal fault location for multi-terminal lines.

A fault location for multi-terminal lines should be implemented in two steps:

1) Detection of faulted line segment.
2) Fault location on faulted line segment using multiple methods.

References

[1] IEEE Std C37.114-2014, IEEE Guide for Determining Fault Location on AC Transmission and Distribution Lines

[2] G. Ziegler, “Numerical Distance Protection: Principles and Application”, Siemens Aktiengesellschaft, 4th Edition, ISBN 978-3-89578-381-4, 2011.

[3] Manual SIPROTEC 5 Distance Protection, Line Differential Protection, and Breaker Management for 1- Pole and 3-Pole Tripping 7SA87, 7SD87, 7SL87, 7VK87, Version V6.00 and higher, SIEMENS AG, C53000- G5040-C011-6
[4] Demetrios A. Tziouvaras, Jeff Roberts, and Gabriel Benmouyal, "New Multi-Ended Fault Location Design for Two- or Three-Terminal Lines", Schweitzer Engineering Laboratories, Inc, 2004

Biographies

Jörg Blumschein studied technical cybernetics and process measurement at the University Magdeburg where he became a graduated engineer in 1992. Since 1992 he works with SIEMENS in the development department of protection relays. Today he is the Principal Key Expert for Protection.

Cezary Dzienis graduated with a degree in Electrical Engineering from Warsaw University of Technology in 2003. He then worked for university's Division of Industrial Electronics and Control System until 2004. Since then, he worked for Chair of Electric Power Networks and Renewable Energy Sources at the University of Magdeburg where he completed his Ph.D. in 2007. From 2008 to 2021 he worked as a researcher in area of protection algorithms at Siemens Berlin. Since 2022 he is a Professor at the University of Applied Sciences Zittau/Görlitz on the Chair of Power System Protection and Network Operation.

Jens Hauschild graduated with a degree in Electrical Power Systems from Technical University Dresden in 1988. Since 1988 he worked in different positions at 50 Hertz Transmission in the field of protection and control. Since 2021 he is heading the department technical concepts. Beside this Jens is active in several groups of VDEW, DKE, FNN and ETG related to the subject of protection and control.